Biochemistry and Biophysics Reports 26 (2021) 100922

Contents lists available at ScienceDirect

Biochemistry and Biophysics Reports

journal homepage: www.elsevier.com/locate/bbrep

Biochemical properties of a native β-1,4-mannanase from *Aspergillus aculeatus* QH1 and partial characterization of its N-glycosylation

Liqing Ma [a], Heping Jiang [a], Weihua Li [b], Hua Qin [c], Zhi Lv [a], Jiujiu Huang [a], Xuewen Hou [a,**], Weijun Wang [a,d,*]

[a] College of Life Sciences, South China Agricultural University, Guangzhou, 510642, China
[b] National Center of Biomedical Analysis, Beijing, 100850, China
[c] Department of Restorative Dentistry, School of Dentistry, Oregon Health & Science University (OHSU), Portland, OR, 97239, USA
[d] Department of Animal Biosciences, University of Guelph, Guelph, Ontario, N1G 2W1, Canada

ARTICLE INFO

Keywords:
β-mannanase
Fungus
N-glycosylation
N-glycan type
N-glycosylation site

ABSTRACT

N-glycosylation plays critical roles in protein secretion, sorting, stability, activity modulation, and interactions to other molecules in the eukaryotic organisms. Fungal β-1,4-mannanases have been widely used in the agri-food industry and contribute to the pathogenesis on plants. However, the information on N-glycosylation of a specific fungal carbohydrate-active enzyme (CAZyme) is currently limited. Herein, a cDNA was cloned from *Aspergillus aculeatus* QH1, displaying a full length of 1302 bp with an open reading frame of 1134 bp encoding for a GH5 subfamily 7 β-1, 4-mannanase, namely AacMan5_7A. The enzyme was purified and exhibited an optimal activity at pH 4.6 and 60 °C, hydrolyzing glucomannan and galactomannan, but not yeast mannan. AacMan5_7A is an N-glycosylated protein decorated with a high-mannose type glycan. Further through UPLC-ESI-MS/MS analysis, one of the four predicted N-glycosylation sites at N255 position was experimentally verified. The present study expands the information of N-glycosylation in fungal CAZymes, providing scientific bases for enhancing the production of fungal enzymes and their applications in food, feed, and plant biomass conversions.

1. Introduction

N-linked protein glycosylation represents the covalent attachment of oligosaccharides (N-glycans) to a nitrogen atom, usually the N^4 of asparagine residues in proteins [1]. In general, there are three types of mature N-glycans, including high-mannose, hybrid and complex. They decorate on many secreted and membrane-bound glycoproteins often at Asn-X-Ser/Thr sequons and occasionally at Asn-X-Cys [1]. N-glycosylation is the most prominent protein co-/post-translational modification in the eukaryotic organisms, and plays many critical roles for both protein structure and function, such as protein sorting, quality control, and secretion [1,2]. The N-glycosylation also affects protein folding, enzyme activity, solubility and stability, and the interactions with other molecules (e.g. lectins and peptide: N-glycosidase) [3,4]. Saprophytic or plant-pathogenic fungi secret an array of carbohydrate–active enzymes (CAZymes) to degrade a wide range of plant cell wall biomass through synergistic actions [5], where N-glycosylation was revealed as the prevalent modification for the secretomes from *Aspergillus* species through glycoproteomic approaches [6,7]. In comparison, the information regarding both glycan type and glycosylation site for a specific fungal carbohydrate-active enzyme (CAZymes) is limited with a focus on cellobiohydrolases [8–10], acetylxylan esterase [11], glucoamylase [12–14]. This information is crucial for the understanding in structure and function of protein glycosylation, and further enhancing the production of fungal enzymes and their applications in feed, food, and plant biomass conversions.

Hemicellulose is the second most abundant plant cell wall polysaccharides after cellulose on the earth. As one of the major hemicellulosic components, β-mannan is the β-(1 → 4)-linked polysaccharides containing D-mannopyranosyl residues (D-Man*p*), whose backbones may consist merely of D-Man*p* (e.g. linear β-mannans), or of D-Man*p* and D-glucopyranosyl (D-Glc*p*) in a non-repeating pattern (e.g. glucomannans). Moreover, the backbone of D-Man*p* residues can be partially substituted with α-(1 → 6)-linked D-galactopyranosyl (D-Gal*p*) group (e.g. galactomannans and galactoglucomannans), as well as acetyl groups at C-2 or/and C-3 positions to different degrees depending on the

* Corresponding author. College of Life Sciences, South China Agricultural University, Guangzhou, 510642, China.
** Corresponding author.
E-mail addresses: hxw1969@scau.edu.cn (X. Hou), weijun@uoguelph.ca (W. Wang).

https://doi.org/10.1016/j.bbrep.2021.100922
Received 26 June 2020; Received in revised form 21 December 2020; Accepted 11 January 2021

source [15,16]. Given this structural heterogeneity, the complete enzymatic hydrolysis of β-mannans requires the concerted action of multiple enzymes, including endo-β-1,4-mannanase (EC.3.2.1.78), endo-β-1,4-glucanase (EC.3.2.1.4), β-1,4-D-mannosidase (EC.3.2.1.78) and/or exo-β-1,4-D-glucosidase that target at the backbone; α-galactosidases (EC 3.2.1.22) and acetyl β-mannan esterases that are required to remove the substituent groups. Among these enzymes, (endo)-β-1,4-D-mannanase randomly hydrolyzes β-(1 → 4)- D- Man*p* linkage in the backbone of β-mannan, and is currently classified into GH families of 5, 26, 113 and 134 based on the similarity of amino acid sequence [17,18]. The fungal β-1,4-D-mannanases not only have a broad range of applications in food, feed, oil drilling, pulp and paper industries [16,19,20], also play important roles in the pathogenesis on plants [21–23]. Fungal endo-β-1,4-mannanases have been isolated and biochemically characterized from *Aspergillus niger*, *Chrysonilia sitophila*, *Pencillium chrysogenum* and others [18]. In particular, β-1,4-mannanases from *A. aculeatus* strains have been recombinantly expressed in *Saccharomyces cerevisiae* [24], *Aspergillus niger* [25] and *Yarrowia lipolytica* [26], and some of their biochemical properties have been reported.

Through the activity-based screening with chromogenic Azo-Xylan, a xylanase-producing fungal strain was isolated from soil, and further identified as *Aspergillus aculeatus* based on its morphology and the partial sequence of 28S ribosomal DNA gene (GenBank accession number: MN396388). Accordingly, it was named as *Aspergillus aculeatus* QH1 [27]. *A. aculeatus* is classified into the Nigri section in the genus of *Aspergillus,* and has shown great potential in producing multiple carbohydrate–active enzymes (CAZymes) for the application in food and feed industries [5,28]. Consistently, *A. aculeatus* QH1 exhibited substantial activities of xylanase, cellulase and β-1,4-mannanase in the solid-state fermentation [27]. The present work aims to gain the structural information for the N-glycosylation in a fungal β-1,4-mannanase. A cDNA encoding for an acidic β-1,4-mannanase (AacMan5_7A) was cloned from *Aspergillus aculeatus* QH1 strain along with its biochemical characterization. In particular, the N-glycosylation of AacMan5_7A was partially investigated for its N-glycans type and N-glycosylation sites. These results will aid in the understanding of glycosylation in eukaryotic organisms.

2. Materials and methods

2.1. Materials and chemicals

Yeast mannan, guar gum, Konjac glucomannan, locust bean gum (LBG), Congo Red and Schiff reagent were all purchased from Sigma-Aldrich. Immobilized WGA- Agarose was from Vector Laboratories (Shenzhen, China); Con A-Sepharose 4B, Phenyl-Sepharose 6 Fast Flow (High Sub) and DEAE-Sephadex were from GE Health Sciences (Guangzhou, China). Endoglycosidase H (Endo-H) from *Streptomyces plicatus* was purchased from New England Biolabs (Beijing, China). SMART™ RACE cDNA amplification kit was purchased from Clontech (Beijing, China). Low molecular weight protein standards were from the Shanghai Institute of Biochemistry. RNeasy Plant Mini Kit was from Qiagen (Beijing, China). Takara PCR cleanup and gel extraction kit were from Takara Bio (Guangzhou, China). The sequence grade modified trypsin was purchased from Roche (Beijing, China). The Konjac flour (75.6% carbohydrate, 7.3 crude protein, 11.2% moisture, 2.3% Ash) and soybean meal were provided by the courtesy of Bosar Biotech Co. Ltd. (Guangzhou, China). All other reagents were of analytical grade. The fungal strain of *Aspergillus aculeatus* QH1was isolated from the soil on the campus of South China Agricultural University. The sequence of partial 28S rRNA gene from *Aspergillus aculeatus* QH1was deposited in GenBank with an accession number of MN396388.

2.2. The cloning of AacMan5_7A cDNA through RACE approach

Aspergillus aculeatus QH1 was grown in 50 mL liquid medium pH 6.0 at 180 rpm in a shaker incubator with an inoculum of 0.5 mL spore suspension solution under 30 °C. The growth medium contained NH_4NO_3 0.6% (w/v), peptone 2.4% (w/v), yeast extract 0.1% (w/v), D-mannose 1.0% (w/v), $MgSO_4$ 0.02% (w/v), KH_2PO_4 0.1% (w/v), KCl 0.05% (w/v), $FeSO_4{\cdot}7H_2O$ 0.001% (w/v). After 5 days cultivation, the mycelium was harvested by centrifugation (6000 g, 15 min) and then grounded using polypropylene pestles in a 1.5 mL microtubes with liquid nitrogen. The total RNA was isolated from grounded samples using the Qiagen RNeasy Plant Mini Kit (Guangzhou, China) according to the manufacturer's protocol for the filamentous fungi and used for the subsequent steps.

The rapid amplification of cDNA ends (RACE) method was employed to obtain the full-length of *AacMan5_7A* cDNA using SMART™ RACE cDNA Amplification Kit. First, the 3′- and 5′- RACE-Ready first strand cDNA were synthesized according to the kit user manual using the extracted total RNA from *Aspergillus aculeatus* QH1. The following gene specific primers (GSPs) were designed according to the conserved regions of known fungal GH5 β-1,4-D-mannanase amino acid sequences. The nested degenerate PCR primers used for the downstream 3′-RACE are GSP2: 5′-GGNCTSCARCGNMTBGACTA-3′ and NGSP2: 5′-GGHGAHGAGGGCWTBGG-3′; and the nested degenerate PCR primers for 5′-RACE are GSP1: 5′-BVKBNCCRTACTgCCAg-3′ and NGSP1: 5′-TCVARNARRCRNggCTT-3′. For both nested PCRs, the first round PCR product was diluted by 50 times, and then used as a template for the second round PCR. The final PCR amplified fragments were then purified with Takara agarose gel DNA purification kit and were ligated to the pMD19-T vector using TA cloning. The inserts were sequenced at Guangzhou IGE Biotechnol Ltd (Guangzhou, China), and the full length of *AacMan5_7A* cDNA was assembled using the online tool of EGassembler (https://www.genome.jp/tools/egassembler/). This assembled *AacMan5_7A* cDNA sequence was deposited in GenBank with an accession number of MN275950, and its coding amino acid sequence was deposit as QEX95509.

2.3. Sequence analysis and N-glycosylation site prediction

The open reading frame (ORF) in the cDNA sequence was identified with the ORF finder at National Center for Biotechnology Information (NCBI; www.ncbi.nlm.nih.gov/projects/gorf/). Modularity and signal peptide of the enzyme was predicted by Simple Modular Architecture Research Tool (SMART; http://smart.embl-heidelberg.de). N-glycosylation sites were predicted using the online tool of NetNGly (http://www.cbs.dtu.dk/services/NetNGlyc/). The sequences were aligned using Clustal W in Geneious 8.0. (Biomatters Ltd, New Zealand) prior to constructing a neighborhood-joining tree using Geneious Tree Builder.

2.4. Solid-state fermentation

Potato dextrose agar (PDA) medium in flat glass bottles was inoculated with *A aculeatus* QH1 spores and incubated at 28 °C for 6 days. The spore suspension was then prepared by washing the agar surface with 20 mL sterile distilled water containing Tween-80 0.05% (v/v) and glycerol 45% (v/v). The concentration of spore suspension was determined to be ~2.24×10^5 spores/mL, and it was used as inoculums for the following solid-state fermentation. The solid-state fermentation was carried out in a 250 mL Erlenmeyer flask containing 10.0 g konjac flour, 4.0 g soybean meal, 0.084 g NH_4NO_3, 0.336 g peptone, 0.014 g yeast extract and 56 mL Vogel's minimal growth medium at pH 6.0. Each flask was inoculated with 1.0 mL of the spore suspension and incubated at 28 °C for 5 days.

2.5. Enzyme extraction and purification

Crude enzyme was extracted from the aforementioned solid-state fermentation in each flask using 50 mL sodium acetate buffer (20 mM, pH 5.0) by oscillations with 10 glass beads (Φ: 5.0 mm) at a shaking

speed of 180 rpm for 1.0 h under 4 °C. The solid residues were first removed using a nylon cloth (200 meshes) filtration. The liquid fraction was collected and centrifuged (6000 g, 15 min) at 4 °C to further remove solid residue. The solid $(NH_4)_2SO_4$ powder was then gradually added to the supernatant to reach a final saturation of 85% and kept at 4 °C overnight. The precipitation was collected by centrifugation (6000 g, 15min), and then dissolved in 10 mL 20 mM pH 5.0 sodium acetate buffer. The resulted solution was centrifuged again and the supernatant was collected.

The supernatant was then loaded into a Sephadex G-75 column (3.0 cm × 45.0 cm) for gel filtration using 20 mM pH 5.0 HAc-NaAc buffer with a flow rate of 1.0 mL/min. The fractions with the β-mannanase activity were collected, adjusted to a final $(NH_4)_2SO_4$ concentration of 0.5 mol/L and loaded to a Phenyl-Sepharose 6 Fast Flow (High Sub) column (2.0 × 8.0 cm). The column was then eluted with a linear $(NH_4)_2SO_4$ gradient from 0.5 mol/L to 0 mol/L in 20 mmol/L sodium acetate buffer (pH 5.0) for 10-column volume. The fractions with the β-mannanase activity were collected and concentrated with the Amicon® stirred ultrafiltration cell (Millipore) using a polyethersulfone membrane (molecular weight cutoff, 10,000 Da; Millipore), and dialyzed against 20 mM pH 5.0 sodium acetate buffer with a dialysis tubing (2000 NMWCO) under 4 °C overnight. Lastly, the dialyzed enzyme was loaded into the DEAE-Cellulose DE52 anion exchange column (3.5 cm × 25.0 cm), eluting with a linear NaCl gradient from 0 mol/L to 0.5 mol/L in 20 mM pH 5.0 sodium acetate buffer for 10-column volume. The fractions with the β-mannanase activity were harvested, concentrated, and stored under −80 °C. Chromatography was performed on a BioLogic LP System (Bio-Rad) at room temperature.

2.6. Enzyme activity assays

The hydrolytic activity of AacMan5_7A on different polysaccharides was examined by measuring reducing sugars release from substrates using the dinitro-salicylic acid (DNS) method [29]. Specifically, enzyme activity assay solution includes 5 mg/mL (0.5%, w/v) polysaccharide substrate in 0.1 M sodium acetate buffer pH 4.6 with a final volume of 1.0 mL. The reaction was initiated by adding an amount of enzyme determined to release products in a linear relation to time when incubated at 65 °C for 10 min. The reaction was terminated by adding 1.5 mL of DNS solution and followed by an incubation at 100 °C for 15 min. The absorbance at a wavelength of 540 nm was measured using Pharmacia Ultrospec 2000 UV/VIS Spectrophotometer. One enzyme activity unit (U) was defined as the amount of enzyme that is required to release 1.0 μmole of D- (+)-mannose equivalent from the tested substrate per minute under standard activity assay conditions. D-(+)-mannose was used to generate a standard curve. All enzyme activity assays were performed in triplicate. Kinetic parameters were calculated using Sigma Plot (Version 10) to fit data with the Michaelis-Menten equation.

In the binding assay with the immobilized lectins, the activity of AacMan5_7A was also measured with the modified gel-diffusion assay [30]. Briefly, the substrate agar solution contained 0.5% (w/v) locust bean gum and 1.5% (w/v) agar in 100 mmol/L pH 4.6 sodium acetate buffer. After autoclaving, this solution was poured into petri dishes (100 mm × 15 mm, 15 mL/plate) to prepare substrate-agar plate for gel-diffusion assay. Sample loading wells were created using 20–200 μl pipette tips, and 1.0 μL enzyme solution was added into each well and incubated under 40 °C for 5 h. Then, the substrate-agar plate was stained with 1.0% (w/v) Congo Red solution for 15 min and rinsed 2 to 3 times with 1.0 mol/L NaCl. The diameter of the clearing zone was measured for quantifying enzyme activity, where the clearing zone diameter is linearly related to the log of enzyme units loaded. All enzyme activity assays were performed in triplicate. The GH5 endo-1,4-β-mannanase from *Bacillus circulans* (400U/mL; Megazyme) was used as a standard for activity calibration.

2.7. Protein assay and SDS-PAGE analysis

Protein concentrations were determined by the Bradford assay using bovine serum albumin as a standard protein [31]. SDS-PAGE was performed and stained with Coomassie Blue according to the established procedures [32].

2.8. PAS staining and endo-H treatment to identify protein glycosylation

Periodic acid/Schiff (PAS) staining was used to detect the glycosylated protein as described previously [33]. Briefly, the purified AacMan5_7A was analyzed by SDS-PAGE (10.0%) first. The gel was fixed with acetic acid/methanol/water (V: V: V = 10:35:55) solution for 1.0 h, and then soaked in 1.0% (v/v) periodic acid solution for 1.0 h. After rinsing with 10.0% (w/v) sodium sulfite solution for 10 min twice, the gel was then placed in Schiff reagents until a magenta band appeared without any further increase in the band intensity. The enzymatic N-deglycosylation of AacMan5_7A was conducted using endoglycosidase H (Endo-H). Briefly, 20 μg of AacMan5_7A in 20 μL total reaction volume containing 1.0 × GlycoBuffer was mixed and incubated with 3.0 μL Endo-H (500,000 units/mL) under 37 °C for 12 h. The Endo-H treated AacMan5_7A was then analyzed by SDS-PAGE (10.0%) along with native AacMan5_7A.

2.9. Binding assay using the immobilized lectins to determine the N-glycans type

The immobilized lectins of ConA-Sepharose 4B and WGA-Agarose (0.5 mL) were packed in glass chromatography columns (1.3 cm × 10.0 cm) respectively and equilibrated with 20 mmol/L sodium acetate buffer pH 6.0 containing 0.5 mol/L NaCl. The purified AacMan5_7A in 0.5 mL in 20 mmol/L sodium acetate buffer pH 6.0 (1.2 mg protein/mL) was loaded to each column with a flow rate of 0.1 mL/min. The flow-through was collected, and each column was then washed with 30 mL of 20 mmol/L sodium acetate buffer pH 6.0 containing 0.5 mol/L NaCl. The enzyme bound to Con A-Sepharose was eluted with 0.5 mol/L α-methyl-mannose in 20 mmol/L sodium acetate buffer pH 6.0. While, the enzyme bound to WGA-agarose was eluted with 0.5 mol/L N-Acetyl-D-Glucosamine (GlcNAc) in the same buffer. The β-mannanase activity in flow-through and eluted samples were measured with the modified gel-diffusion assay.

2.10. Protein in-gel digestion

Protein in-gel digestion was performed as described previously with some modifications [34]. Briefly, the Coomassie Blue R-250 stained protein bands in SDS-PAGE gel for the native and N-deglycosylated AacMan5_7A by Endo-H were excised using a clean razor blade, respectively. The gel pieces were destained with 200 μl of 50 mmol/L ammonium bicarbonate in 50% (v/v) acetonitrile (ACN) for 20 min for 3 times. The gel pieces were dried in a SpeedVac vacuum system (Savant Instruments, Holbrook, NY, USA), and then rehydrated with 10.0 μl sequence grade modified trypsin solution (10 ng/μl) in 25 mmol/L ammonium bicarbonate solution pH 8.0 under 4 °C for 40 min. An additional 25 mmol/L ammonium bicarbonate solution of 10 μl was added for 12.0 h digestion under 37 °C. The peptide was extracted with 100 μl 5% (v/v) trifluoroacetic acid (TFA) at 37 °C for 1 h and followed by the addition of 20 μl of 2.5% (v/v) TFA/50% ACN (v/v) for an incubation at 37 °C for 1 h. The combined extract from the same sample were dried in a SpeedVac concentrator and dissolved in 4 μl of 0.5% aqueous TFA for the subsequent ultraperformance liquid chromatography coupled with tandem and electrospray mass spectrometry analysis (UPLC-ESI-MS/MS).

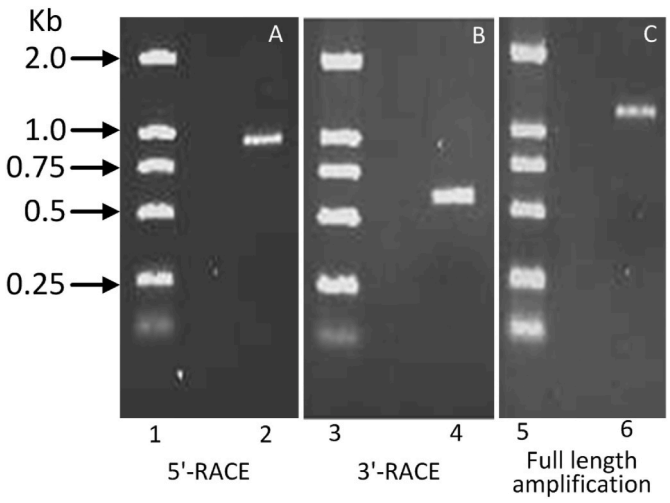

Fig. 1. Agarose gel electrophoresis of the amplified cDNA products of *AacMan5_7A* from *Aspergillus aculeatus* QH1 using SMART-RACE. The concentration of agarose gel was 2.0% (w/v). **A:** 5′-RACE, lane 1: DNA molecular ladder, lane 2: 5′-RACE-PCR products; B: 3′-RACE, lane 3: DNA molecular ladder, lane 4: 3′-RACE-PCR products; C: Full-length amplification, lane 5: DNA molecular ladder, lane 6: full-length PCR product.

2.11. UPLC-ESI-MS/MS

Analysis UPLC-ESI-MS/MS was carried out using the nanoACQUITY UPLC system linked to an electrospray ionization-MS/MS system (Waters Synapt High Definition Mass Spectrometry) at National Center of Biomedical Analysis, Beijing, China Tryptic peptides from native and Endo-H treated AacMan5_7A were separated with a 5 μm, 20 mm × 180 μm Symmetry C_{18} pre-column, and a 1.7 μm, 250 mm × 75 μm BEH C_{18} column (Waters) using the nanoACQUITY UPLC system. The samples were loaded with 0.1% (v/v) aqueous formic acid (solvent A) for 4 min. The peptides were eluted with a binary solvent system of solvent A and solvent B [0.1% (v/v) formic acid in ACN] using a linear gradient of 1.0%–40.0% of solvent B over 10 min, followed by a second linear gradient from 40% to 80% of solvent B over 10 min, a rinse for 10 min with 90% solvent B and re-equilibration at initial conditions for 20 min. The flow rate was kept at 0.2 mL/min, and the column temperature was maintained at 35 °C.

For all measurements, the Synapt HD-MS system was operated in the v-mode with a typical resolving power of at least 10,000 full-width at half-maximum. The time-of-flight analyzer of the mass spectrometer was calibrated with the MS/MS fragment ions of [Glu-1]-Fibrinopeptide B from m/z 50 to 2600. The reference sprayer was sampled at a frequency of 30 s. Accurate UPLC-MS/MS data were collected in data-dependent analysis mode by performing MS/MS scans (2-s duration) for the two most intense peaks from each MS scan (1-s duration). Peak lists were generated using ProteinLynx Global Server software version 2.3 (Waters) and automatically combined into a single pkl file for every UPLC-MS/MS run for the database search. The mass accuracy of both MS and MS/MS is below 0.2 Da. Peptide *de novo* sequencing was performed using Biolynx software (Waters).

2.12. Homology modeling in 3-D structure

The 3-dimensional model of AacMan5_7A β-1,4-mannanase was generated by the SWISS-MODEL online server for the residues from 13 to 354, using the crystal structure of a β-1,4-mannanase from *Aspergillus niger* BK01 (PDB ID: 3wh9, sequence identity of 75%) as a template. The structure model was analyzed and visualized using PyMOL 2.1 (www.pymol.org).

3. Results and discussion

3.1. A cDNA encoding β-1, 4-mannanase was cloned from Aspergillus aculeatus QH1

The cDNA encoding a β-1,4-mannanase from *A. aculeatus* QH1 was cloned using the rapid amplification of cDNA ends (RACE) approach. Specifically, 5′- and 3′- RACE generated 1.0 kb and 0.6 kb fragments respectively (Fig. 1-A, B). These two fragments were sequenced and assembled into a cDNA sequence for a full length of 1302 bp (GenBank accession number: MN275950), which exactly matched with the sequence of a fragment from full-length PCR amplification (Fig. 1-C). Overall, this cDNA contains an open reading frame (ORF) of 1134 bp flanked by a 36-bp long 5′-untranslated region and a 132-bp long 3′-untranslated region that includes a poly (A) tail. This ORF encodes a protein of 373 amino acids (GenBank accession number: QEX95509) containing a signal peptide sequence at the N-terminus (1–18 amino acids), displaying an amino acid sequence identity of 97.3% to a previously reported GH5_7 (glycohydrolase family 5 subfamily 7) β-1,4-mannanase from *Aspergillus aculeatus* (Uniprot number: Q00012) (Christgau et al., 1994) and with the closest homologue being a putative GH5_7 endo-1,4-β-mannosidase A (XP_025527873) from *Aspergillus indologenus* CBS 114.80 (amino acid sequence identity of 98.9%). The molecular size of this mature β-1,4-mannanase (with the signal peptide sequence of 1–18 amino acids removed) is predicted to be 39.18 kDa without any post-translational modifications. Furthermore, the phylogenetic analysis with the amino sequences of the characterized GH5 enzymes from CAZyme database revealed that this β-1,4-mannanase sequence is clustered with the current subfamily 7 sequences in GH5 family (Fig. S1) (CAZyme database, http://www.cazy.org), and thus belongs to subfamily 7 in GH5 family [36]. Therefore, this enzyme was named as AacMan5_7A. Consistently, the most of the previously reported GH5 β-1,4-mannanases are classified into subfamily 7 and 8 with the exception of some other members belonging to subfamily 10 and 17 [36]. Within the GH5_7 subfamily, the catalytic domains of β-1,4-mannanases are often associated with carbohydrate-binding modules (CBM), such as CBM1, CBM5, CBM27 and CBM10 (Table S1), whereas, no canonical CBM is recognizable in the AacMan5_7A sequence, and thus this enzyme is a mono-modular β-1,4-mannanase. The mono-modularity and relatively small molecular size of AacMan5_7A might be beneficial for its application in feed and plant biomass conversion, given the favor to the enzyme penetration into lignocellulosic biomass [37,38].

3.2. The biochemical properties of the acidic β-1, 4-mannanase from Aspergillus aculeatus QH1

In parallel with the cDNA cloning, a β-1, 4-mannanase was purified from the solid-state culture of *A. aculeatus* QH1 by 9.2 times with a total activity recovery of 32.6% (Table S2). The purified enzyme showed a single protein staining band in SDS-PAGE with a molecular size of 42.1 kDa (Fig. S2). This purified enzyme was confirmed to be AacMan5_7A by the amino acid sequence of its peptide fragment using tandem MS (MS/MS) analysis, which was identical to the sequence of AacMan5_7A (GenBank accession number: QEX95509) from amino acid 243 to 258) (Also see section 3.4 below). Hereafter, this β-1, 4-mannanase was referred to as AacMan5_7A.

AacMan5_7A exhibited an optimum activity at pH 4.6 (Fig. S3-A) and 60 °C when the locust bean gum was used as the substrate (Fig. S3-C), which is similar to the previously reported optimum reaction pH and temperature at 5.0 and 60~70℃ for a recombinant β-1, 4-mannanases from *A. aculeatus* when expressed at *A. oryzae* [35]. In addition, it is around 1.5 pH unit higher than the previously reported optimum reaction pH at 3.0–3.8 for the β-1, 4-mannanases from *A. aculeatus* MRC11624 [24–26]. This difference is likely due to the slightly different amino acid sequence between two enzymes and different buffers used for activity assay. Similarly, most of the fungal β-1, 4-mannanase

Table 1
Substrate specificity of an acidic β-1,4-mannananse from *Aspergillus aculeatus* QH1.

Substrate	Chemical composition	Specific activity (U/mg)	$K_{m(app)}$ (mg/mL)	V_{max} ($\times 10^3$ U/mg)	$V_{max}/K_{m(app)}$
Konjac mannan	Glucomannan	1605.3 ± 12.5	0.85 ± 0.13	2.59 ± 0.34	3047.1
locust bean gum	Galactomannan	2037.4 ± 2.9	1.19 ± 0.23	2.45 ± 0.41	2058.8
Guar gum	Galactomannan	1433.1 ± 17.0	3.38 ± 0.61	4.35 ± 0.25	1287.0
Yeast mannan	α-(1–6) linked D-Man*p* backbone and α-(1–2) and α-(1–3) linked D-Man*p* substituents	ND*			

*ND:No detectable activity. The activity assay was performed in 0.1 M HAc-NaAc buffer (pH 4.6) with a final volume of 1.0 mL at 65 °C for 10 min. All enzyme activity assays were performed in triplicate. Kinetic parameters were calculated by using Sigma Plot to fit data with the Michaelis-Menten equation. The concentration of the substrate for specific activity assay was at 0.5% (w/v). No activity was detectable for AacMan5_7A towards birch xylan, chitin, and chitosan.

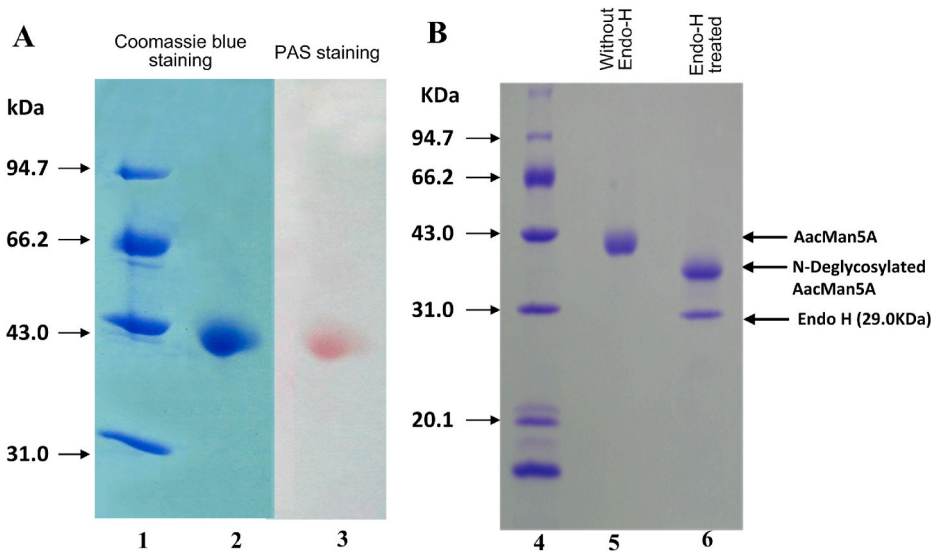

Fig. 2. The PAS staining and Endo-H digestion revealed N-linked glycosylation for AacMan5_7A. A: The PAS staining after SDS-PAGE revealed the glycosylation of AacMan5_7A; lane 1: protein standard with Coomassie Blue staining; lane 2: the purified AacMan5_7A after Coomassie Blue staining; lane 3: the purified AacMan5_7A after PAS staining, and showed as a magenta band. **B:** The N-deglycosylation of AacMan5_7A by Endo-H treatment showed a decrease in molecular size from 42.1 to 38.7 kDa by ~3.4 kDa lane 4: protein standard; lane 5: the purified AaMan5_7A; lane 6: the purified AacMan5_7A after Endo-H treatment.

displayed acidic pH optimum for their activities [18]. The enzyme retained >60% of its maximum activity from pH 3.0–7.5 (Fig. S3-B). The half-life of AacMan5_7A under 60 °C was around 40 min and decreased to 5 min under 70 °C (Fig. S3-D). Similar to the previous report [24], the AacMan5_7A displayed the highest specific activity of 2037 U/mg towards locust bean gum (galactomannan), followed by Konjac glucomannan and guar gum (galactomannan) (Table 1). However, no activity was detected towards yeast mannan and β-(1 → 3) (1 → 4)-glucan, indicating that AacMan5_7A specifically cleave β-(1 → 4)-D-Man*p* linkage within these tested polysaccharides. The presence of 5.0 mM Cd^{2+}, Hg^{2+} and Co^{2+} significantly reduced activity of AacMan5_7A by 50–70% (Table S3), which is similar to the previous report for a β-1, 4- mannanase from *Aspergillus niger* [39].

Given the polydispersity of plant cell wall polysaccharides (e.g. the glucomannan and galactomannan), molar values of these substrates could not be accurately calculated, and thus, only apparent kinetic parameters (e.g. $K_{m(app)}$) could be obtained to evaluate enzyme activity [40]. Herein, the AacMan5_7A activity towards Konjac glucomannan displayed the highest catalytic efficiency coefficient ($V_{max}/K_{m(app)}$), followed by locust bean gum and guar gum (both are galactomannan), reflecting a slight steric hindrance effect of α- (1 → 6)-galactose substituents in enzyme catalysis (Table 1).

3.3. AacMan5_7A β-1, 4-mannanase is a N-glycosylated protein decorated with a high-mannose-type glycan

Protein N-glycosylation plays many critical roles for the secretion, functionality and properties of enzymes from the eukaryotic organisms [2]. In this study, the PAS staining revealed a magenta band for AacMan5_7A after SDS-PAGE (Fig. 2-A), suggesting that AacMan5_7A is a glycosylated protein. Afterward, AacMan5_7A was treated with Endo-H to further probe its glycosylation type. Endo-H specifically cleaves β-(1 → 4) glycosidic linkage between two N-acetylglucosamine (GlcNAc) residues in the chitobiose core of N-linked high-mannose or some hybrid glycans, remaining one N-acetylglucosamine residue (N-GlcNAc) attached to the asparagine residue. Herein, the Endo-H treatment reduced molecular size of AacMan5_7A from 42 kDa to 39 kDa by ~3 kDa as shown in SDS-PAGE (Fig. 2-B), indicating that AacMan5_7A is an N-glycosylated protein. Consistently, the recombinant and native β-1, 4- mannanase from *Aspergillus aculeatus* MRC 11624 have also been shown as a N-glycosylated enzyme with the PNGase F treatment [24]. However, the information regarding N-glycan type and N-glycosylation sites in fungal β-mannanases is currently not available.

To further understand the type of N-glycan in AacMan5_7A, two immobilized lectins, ConA-Sepharose and WGA-Agarose, were selected to examine their specific binding to N-glycan of enzyme, respectively. It is known that ConA binds to the terminal α-mannose in both high-mannose type and hybrid-type N-glycans; while WGA binds to terminal sialic acid or N-acetyl-glucosamine in hybrid or complex type N-glycans [1]. Our results showed that AacMan5_7A was bound to Con A-Sepharose 4B tightly as it could only be eluted out by 0.5 mol/L α-methyl-mannose solution (Fig. 3-A). In contrast, no binding was observed between AacMan5_7A and WGA-agarose, as the β-mannanase activity remained in the flow-through (Fig. 3-B), ruling out the possibility of the hybrid type glycans being attached to AacMan5_7A. Therefore, the N-glycans attached to the AacMan5_7A surface belongs to high-mannose type. Due to the complexity of a glycan structure, the elucidation of the detail structure of this N-glycan requires future

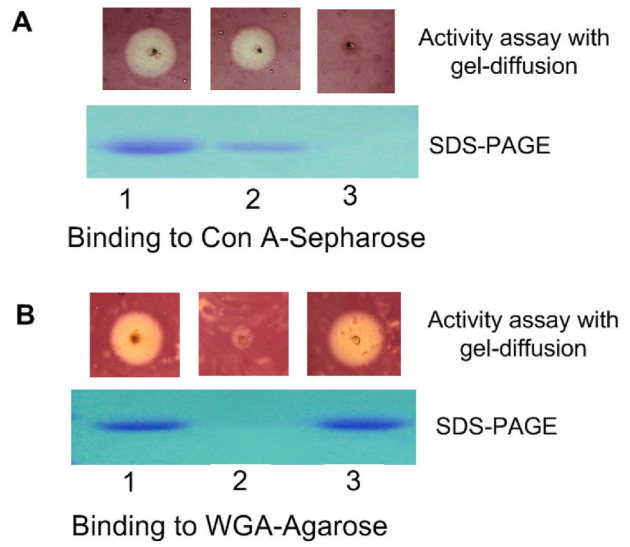

Fig. 3. Specific lectin binding for determining the type of N-glucan attached to AacMan5_7A. The top section is to display the enzyme activity measured by gel-diffusion assay and the bottom section represents the protein samples in SDS-PAGE analysis. **A**: The specific binding of AacMan5_7A to ConA-Sepharose gel; lane 1: The purified AacMan5_7A solution before incubating with ConA-Sepharose; lane 2: the bound AacMan5_7A eluted from ConA- Sepharose by 0.5 mol/L α-methyl-mannose; lane 3: The flow through fraction of enzyme sample from ConA- Sepharose column. B: The specific binding of AacMan5_7A to WGA-agarose gel. Lane 1: The purified AacMan5_7A solution before incubating with WGA-agarose gel; lane 2: the bound AacMan5_7A eluted from WGA-agarose by 0.5 mol/L N-Acetyl-D-Glucosamine (GlcNAc); lane 3: The flow through fraction of enzyme sample from WGA-agarose.

in-depth mass spectrometry-based analysis. Notably, the high-mannose type was also found as predominant N-glycan for a cellobiohydrolase (CBH II) from *Trichoderma reesei* [9]. The type of N-glycan at protein surface is the determinant for the glycoprotein interacting with other molecules such as lectins and N-glycosidase. Relative to mass spectrometry, the immobilized lectin binding assay is a quick and simple approach to determine the general type of N-glycan in glycoproteins.

3.4. One of the four predicted N-glycosylation sites in AacMan5_7A was confirmed

Other than N-glycan type, glycosylation site is another aspect of N-glycosylation. With NetNGlyc online tool (http://www.cbs.dtu.dk/services/NetNGlyc/), four N-glycosylation sites were predicted at N105, N255, N326 and N357 within the amino acid sequence of AacMan5_7A (QEX95509) (Fig. 4-A). Despite of the critical roles of protein N-glycosylation, these predicted N-glycosylation sites are not conserved across the sequences of GH5 fungal β-1, 4-mannanase (Fig. S4). Similarly, the conservation of the N-glycosylation sites was not observed in Aspergilli secreted and homologous proteins [6]. Meanwhile, a homology model was built for AacMan5_7A with an RMSD value of 0.2 Å to the template structure of a homologous β-1,4-mannanase from *Aspergillus niger* BK01 (PDB ID: 3wh9, sequence identity of 75%) (Fig. 4-A). The model displayed a classic $(\beta/\alpha)_8$-(TIM) barrel fold typical for family 5 glycoside hydrolases. By comparing our model with the structure of a GH5 β-mannosidase mutant (RmMan5B E202A) from *Rhizomucor miehei* (PDB ID: 4LYQ) in complex with manno-oligosaccharides, a substrate backbone binding cleft was identified at the C-terminal side of TIM barrel, which likely involves the conserved aromatic amino acid residues of W56, W142. W278 and W336 (Fig. 4-B, Fig. S4). In particular, all of the four predicted N-glycosylation sites were located in the loop regions (Fig. 4-A). It is consistent with the previous report that the N-glycosylation sites were mainly located in the loop regions of protein structures [41]. Furthermore, these four predicted N-glycosylation sites are not located in the surface area close to the catalytic site and substrate binding cleft (Fig. 4-B), implying that the effect of N-glycans on the accommodation for a polymeric substrate in AacMan5_7A is likely minor.

It has been shown that the NXS/T tri-peptide is the predominant motif for protein N-glycosylation, however, not every predicted N-glycosylation site will be occupied [41]. Therefore, the experimental validation of N-glycosylation sites is indispensable for understanding N-glycosylation in the target proteins. Therefore, a comparative MS spectrums analysis for the tryptic peptides from native and Endo-H treated AacMan5_7A was performed using ultra-high-performance liquid chromatography (UPLC) coupled with electrospray tandem mass spectrometry (UPLC-ESI-MS/MS). Relative to native AacMan5_7A, a new and triply charged ion peak ($[M+3H]^{3+}$ (based on its isotopic peak distribution shown in the insert of Fig. 5-B) emerged in the peptide mass spectrum of the N-deglycosylated AacMan5_7A with a mass-to-charge ratio (m/z) of 1223.97, representing a peptide with a molecular mass of 3668.91 Da (Fig. 5A and B). The intensity of this peak was increased dramatically after an endo-H treatment (Fig. 5), suggesting that the emerged $[M+3H]^{3+}$ mass peak corresponded to an N-glycosylated peptide whose glycan was removed by the Endo-H treatment. Indeed, after performing *de novo* sequencing on the MS/MS data of this identified peptide, an amino acid sequence of DGSYPYTYGEGL(N-NAc)^{205}FTK was obtained (Fig. 6). As shown in the spectrum,

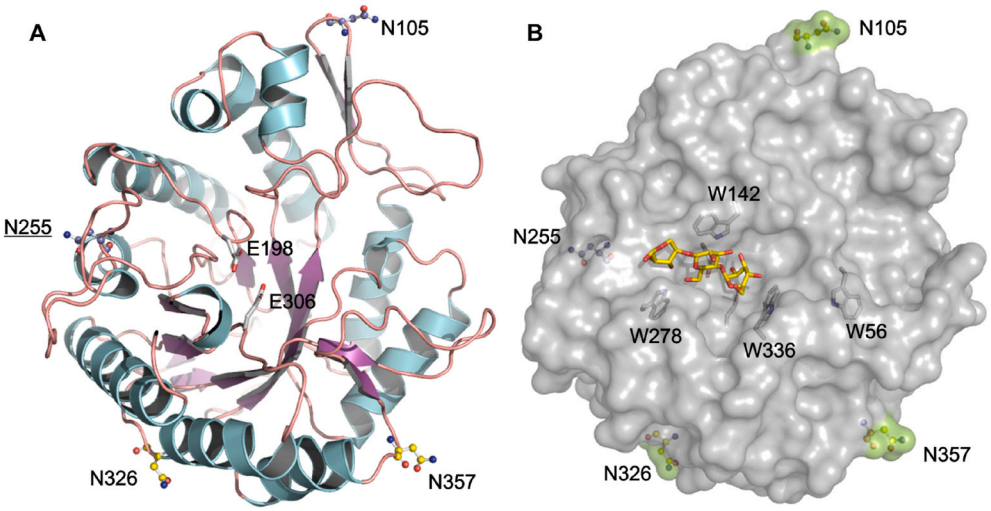

Fig. 4. Three-dimensional model showing predicted and experimentally confirmed N-glycosylation sites of AacMan5_7A. A: Homology models of AacMan5_7A showing catalytic site, predicted, and confirmed N-glycosylation sites. Asparagine residues at N-glycosylation sites were presented as ball and stick. The N-glycosylation site at N-255 (underlined) was experimentally confirmed. **B:** The surface presentation of AacMan5_7A homology model. The amino acid residues likely involving in substrate binding were presented as sticks in grey, and mannotriose was shown as sticks in yellow and red. Asparagine residues at N-glycosylation sites were shown with green surface as well as in balls and sticks. (For interpretation of the references to colour in this figure legend, the reader is referred to the Web version of this article.)

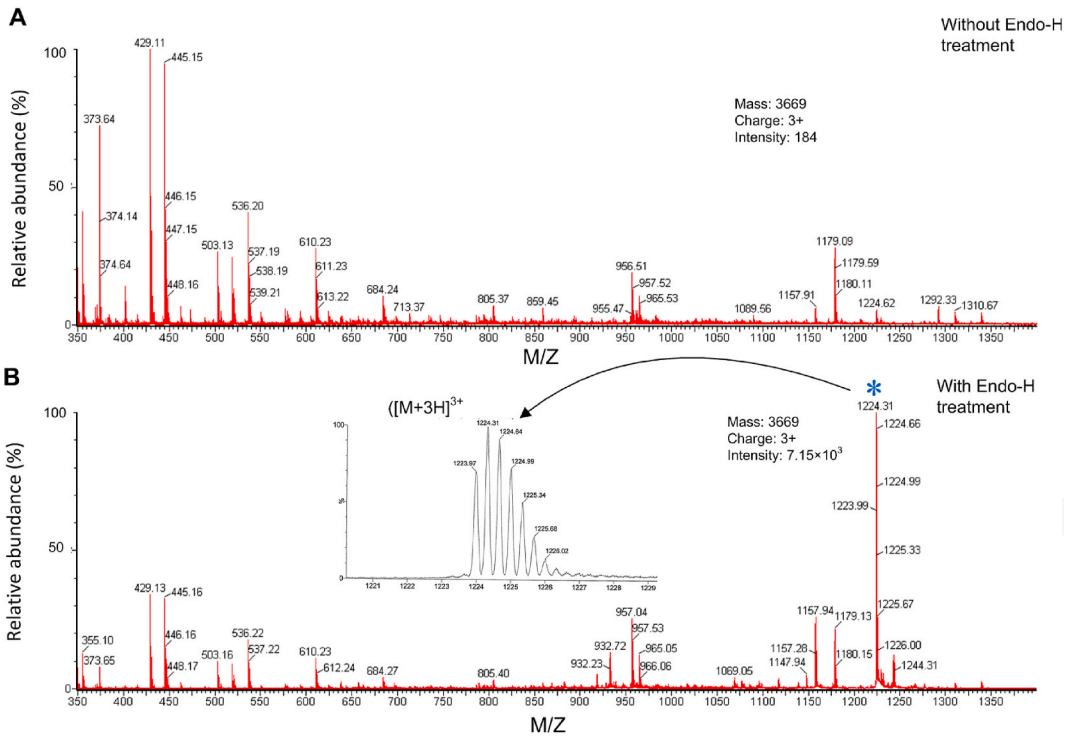

Fig. 5. UPLC-ESI-MS analysis to identify a N-glycosylated peptide from trypsin digestion of AacMan5_7A. A: Mass spectrum of tryptic peptides from the purified native AacMan5_7A after UPLC. **B:** Mass spectrum of tryptic peptides from Endo-H treated AacMan5_7A after UPLC, the emergent mass peak of $[M+3H]^{3+}$ with an m/z ratio of 1223.97 was labelled with star, and its isotopic peak distribution was further shown in the insert.

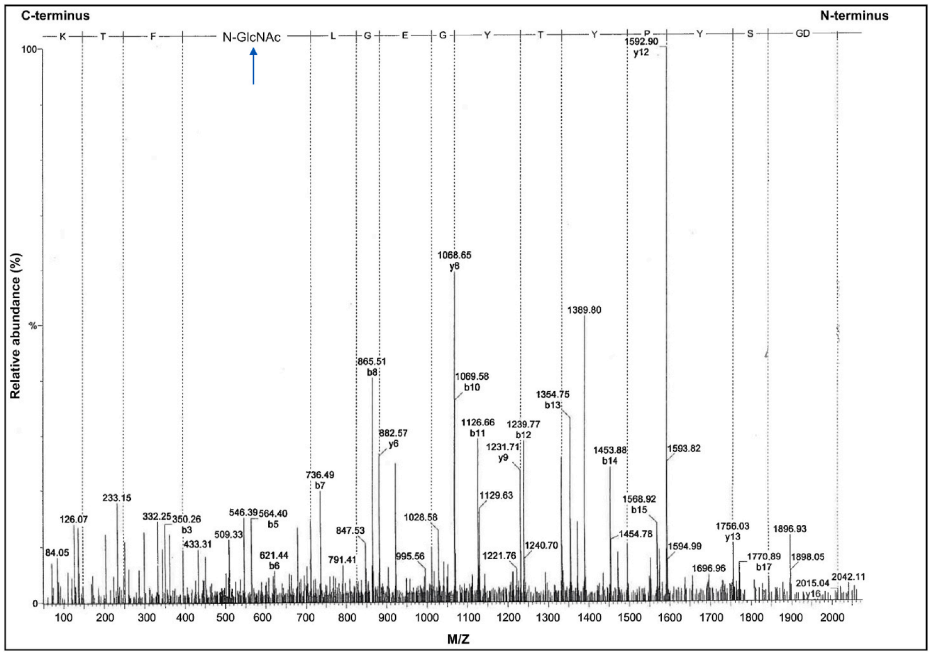

Fig. 6. ESI-MS/MS sequencing of an N-glycosylated peptide from AacMan5_7A. A: *De novo* sequencing with MS/MS for an N-glycosylated peptide from AacMan5_7A. N-GlcNAC indicated with an arrow represents the N-acetyl glucosaminated Asp residue.

an N-glycosylation motif of NFT at Asp255 was found, where the Asp255 attached to an additional NAc after EndoH treatment (Fig. 6). The sequence of this peptide was matched with the amino acid sequence of AacMan5_7A translated from its cDNA in a region from the amino acid residue of 243–258 (GenBank accession number: QEX95509). Consistently, we also detected a peptide signal ($[M+3H]^{3+}$) at an m/z of 1156.33 with a molecular mass of 3465.99 Da (data not shown), which differs from the molecular mass (3668.91 Da) of the aforementioned peptide by 203.1Da. This mass difference of 203.1 Da matched with the molecular mass of an N-acetyl glucosamine group (GlcNAc) that was remained to asparagine after Endo-H treatment. This peptide fragment (3668.91 Da) was likely derived from the small portion of non-glycosylated AacMan5_7A or GlcNAc was removed by in-source dissociation.

Notably, the predicted molecular mass for a regular high-mannose Man-5 type N-glycan is 1883.7 Da, which is smaller than the molecular mass difference (i.e. ~3.4 kDa) observed between native and endo-H treated AacMan5_7A by SDS-PAGE (Fig. 3-B). This indicates that at least one additional N-glycosylation site is present in AacMan5_7A. The future analysis using chymotrypsin or other proteases digestion to generate smaller peptide fragments is expected to identify additional N-glycosylation sites. Altogether, the current study has experimentally verified one N-glycosylation site at N255 for AacMan5_7A from *Aspergillus aculeatus* QH1, which is out of the enzyme surface area close to the catalytic site and substrate binding cleft.

4. Conclusion

The present work reports the general enzyme properties and the partial characterization of the N-linked glycosylation for a fungal β-1,4-mannanase from *Aspergillus aculeatus* QH1, including its N-glycan type and N-glycosylation sites. A combined methodology of N-glycosylation analysis using lectin binding assays and mass spectrometry in present study can also be applied to other eukaryotic proteins. Altogether, the current study adds new insights into the knowledge regarding N-glycosylation in fungal CAZymes, and further provides scientific bases to enhance their research, production, and applications in feed, food, and plant biomass conversions.

Author contributions

L.M. and H. J designed and performed experiments, analyzed data, and compiled manuscript. W.L performed UPLC-MS/MS analysis and contributed to writing. H.Q, Z.L and J.H participated in solid fermentation and enzyme characterization. Z.L and J.H. participated in cDNA clone and discussion. X.H contributed to students advising and writing. W.W. conceived, coordinated the study, and compiled manuscript.

Declaration of competing interest

The authors declare no conflict of interest.

Acknowledgements

This research was supported by the grants from the National Natural Science Foundation of China (No. 39900008) and Natural Science Foundation of Guangdong Province (No. 990693) to W. Wang. We would like to thank Dr. Ting Zhou at Guelph Research and Development Center, Agriculture and Agri-food Canada for his comments on the draft of this paper.

Abbreviations

CAZymes	carbohydrate–active enzymes
UPLC-ESI-MS/MS	Automated nanoflow ultra-performance liquid chromatography-electrospray ionization-tandem mass spectrometry analysis
D-Man*p*:	D-mannopyranosyl residue
D-Glu*p*:	D-glucopyranosyl residue
D-Gal*p*:	D-galactopyranosyl residue
GH	Glycoside hydrolase
Endo-H:	Endoglycosidase H from *Streptomyces plicatus*
RACE	the rapid amplification of cDNA ends
ORF	open reading frame
PAS	Periodic acid/Schiff staining
GlcNAc	N-Acetyl-D-Glucosamine;
TFA	trifluoroacetic acid
ACN	acetonitrile

Appendix A. Supplementary data

Supplementary data related to this article can be found at https://doi.org/10.1016/j.bbrep.2021.100922.

References

[1] A. Varki, M.E.E. Richard D Cummings, Jeffrey D. Esko, Hudson H. Freeze, Pamela Stanley, Carolyn R. Bertozzi, Gerald W. Hart, Essentials of Glycobiology, Third, Cold Spring Harbor Laboratory Press, New York, 2009.
[2] M. Molinari, N-glycan structure dictates extension of protein folding or onset of disposal, Nat. Chem. Biol. 3 (2007) 313–320.
[3] A. Helenius, M. Aebi, Intracellular functions of N-linked glycans, Science 291 (2001) 2364–2369, 80.
[4] D. Skropeta, The effect of individual N-glycans on enzyme activity, Bioorg. Med. Chem. 17 (2009) 2645–2653.
[5] M.R. Mäkelä, N. Donofrio, R.P. De Vries, Plant biomass degradation by fungi, Fungal Genet. Biol. 72 (2014) 2–9.
[6] M.V. Rubio, M.P. Zubieta, J. Paulo, L. Franco, F. Calzado, A. Franco, P. Leme, F. M. Squina, R.A. Prade, A. Ricardo, D.L. Damásio, Mapping N - linked glycosylation of carbohydrate - active enzymes in the secretome of *Aspergillus nidulans* grown on lignocellulose, Biotechnol. Biofuels (2016) 1–19.
[7] L. Wang, U.K. Aryal, Z. Dai, A.C. Mason, M.E. Monroe, Z.X. Tian, J.Y. Zhou, D. Su, K.K. Weitz, T. Liu, D.G. Camp, R.D. Smith, S.E. Baker, W.J. Qian, Mapping N-linked glycosylation sites in the secretome and whole cells of *Aspergillus niger* using hydrazide chemistry and mass spectrometry, J. Proteome Res. 11 (2012) 143–156.
[8] G.T. Beckham, Z. Dai, J.F. Matthews, M. Momany, C.M. Payne, W.S. Adney, S. E. Baker, M.E. Himmel, Harnessing glycosylation to improve cellulase activity, Curr. Opin. Biotechnol. 23 (2012) 338–345.
[9] J.P.M. Hui, T.C. White, P. Thibault, Identification of glycan structure and glycosylation sites in cellobiohydrolase II and endoglucanases I and II from *Trichoderma reesei*, Glycobiology 12 (2002) 837–849.
[10] A. Amore, B.C. Knott, N.T. Supekar, A. Shajahan, P. Azadi, P. Zhao, L. Wells, J. G. Linger, S.E. Hobdey, T.A. Vander Wall, T. Shollenberger, J.M. Yarbrough, Z. Tan, M.F. Crowley, M.E. Himmel, S.R. Decker, G.T. Beckham, L.E. Taylor, Distinct roles of N- and O-glycans in cellulase activity and stability, Proc. Natl. Acad. Sci. U. S. A 114 (2017) 13667–13672.
[11] M.J. Harrison, I.M. Wathugala, M. Tenkanen, N.H. Packer, K.M.H. Nevalainen, Glycosylation of acetylxylan esterase from *Trichoderma reesei*, Glycobiology 12 (2002) 291–298.
[12] K.L. Brite Svensson, I. Svendsen, The complete amino acid sequence of the glycoprotein , glucoamylase G1 from *Aspergillus niger*, Carlsberg Res. Commun. 48 (1983) 529–544.
[13] K.L. Brite Svensson, I. Svendsen, Amino acid sequence of tryptic fragments of glucoamylase G1 from *Aspergillus niger*, Carlsberg Res. Commun. 48 (1983) 517–527.
[14] H. Chen, C. Ford, P.J. Reilly, Substitution of asparagine residues in *Aspergillus awamori* glucoamylase by site-directed mutagenesis to eliminate N-glycosylation and inactivation by deamidation, Biochem. J. 301 (1994) 275–281.
[15] H.V. Scheller, P. Ulvskov, Hemicelluloses, Annu. Rev. Plant Biol. 61 (2010) 263–289.
[16] M. Yamabhai, S. Sak-ubol, W. Srila, D. Haltrich, Mannan biotechnology: from biofuels to health, Crit. Rev. Biotechnol. 36 (2016) 32–42.
[17] M. Couturier, A. Roussel, A. Rosengren, P. Leone, H. Stålbrand, J.G. Berrin, Structural and biochemical analyses of glycoside hydrolase families 5 and 26 β-(1,4)-mannanases from *Podospora anserina* reveal differences upon manno-oligosaccharide catalysis, J. Biol. Chem. 288 (2013) 14624–14635.
[18] P.K. Srivastava, M. Kapoor, Production , properties , and applications of endo - β -mannanases, Biotechnol. Adv. 35 (2017) 1–19.
[19] S. Dhawan, J. Kaur, Microbial Mannanases : an overview of production and applications, Crit. Rev. Biotechnol. 27 (2007) 197–216.
[20] L.R.S. Moreira, E.X.F. Filho, An overview of mannan structure and mannan-degrading enzyme systems, Appl. Microbiol. Biotechnol. 79 (2008) 165–178.
[21] J.D. Bewley, Breaking down the walls - a role for endo-β-mannanase in release from seed dormancy? Trends Plant Sci. 2 (1997) 464–469.
[22] S.A. Filichkin, J.M. Leonard, A. Monteros, P.P. Liu, H. Nonogaki, A novel endo-β-mannanase gene in tomato LeMAN5 is associated with anther and pollen development, Plant Physiol. 134 (2004) 1080–1087.
[23] C.P. Kubicek, T.L. Starr, N.L. Glass, Plant cell wall–degrading enzymes and their secretion in plant-pathogenic fungi, Annu. Rev. Phytopathol. 52 (2014) 427–451.
[24] M.E. Setati, P. Ademark, W.H. van Zyl, B. Hahn-Hägerdal, H. Stålbrand, Expression of the *Aspergillus aculeatus* endo- b-1,4-mannanase encoding gene (man1) in *Saccharomyces cerevisiae* and characterization of the recombinant Enzyme, Protein Expr. Purif. 21 (2001) 105–114.
[25] P.J. Van Zyl, V. Moodley, S.H. Rose, R.L. Roth, W.H. Van Zyl, Production of the *Aspergillus aculeatus* endo-1,4-b-mannanase in *A Niger*, J. Ind. Microbiol. Biotechnol. 36 (2009) 611–617.
[26] R. Roth, V. Moodley, P. Van Zyl, Heterologous expression and optimized production of an *Aspergillus aculeatus* endo-1,4- b-mannanase in *Yarrowia lipolytica*, Mol. Biotechnol. 43 (2009) 112–120.
[27] H.(South C.A.U.) Qin, The Screening of Fungal Strains for Xylanase Production and Enzyme Characterization, Master Thesis, South China Agricultural University, 2006.

[28] S. Tani, T. Kawaguchi, T. Kobayashi, Complex regulation of hydrolytic enzyme genes for cellulosic biomass degradation in filamentous fungi, Appl. Microbiol. Biotechnol. 98 (2014) 4829–4837.
[29] G.L. Miller, Use of dinitrosalicylic acid reagent for determination of reducing sugar, Anal. Chem. 31 (1959) 426–428.
[30] B. Downie, H.W.M. Hilhorst, J. Derek Bewley, A new assay for quantifying endo-β-d-mannanase activity using Congo red dye, Phytochemistry 36 (1994) 829–835.
[31] M.M. Bradford, A rapid and sensitive method for the quantitation of microgram quantities of protein utilizing the principle of protein-dye binding, Anal. Biochem. 72 (1976) 248–254.
[32] U.K. Laemmli, Cleavage of structural proteins during the assembly of the head of bacteriophage T4, Nature 227 (1970) 680–685.
[33] R.A. Kapitany, E.J. Zebrowski, A high resolution gel PAS stain for polyacrylamide electrophoresis, Anal. Biochem. 369 (1973) 361–369.
[34] A. Shevchenko, H. Tomas, J. Havli, J. V Olsen, M. Mann, In-gel digestion for mass spectrometric characterization of proteins and proteomes, Nat. Protoc. 1 (2007) 2856–2860.
[35] H. Dalbøge, S. Christgau, S. Kauppinen, J. Vind, L.V. Kofod, Expression cloning, purification and characterization of a beta-1,4-mannanase from *Aspergillus aculeatus*, Biochem. Mol. Biol. Int. 33 (1994) 917–925.
[36] H. Aspeborg, P.M. Coutinho, Y. Wang, H. Brumer, B. Henrissat, Evolution, substrate specificity and subfamily classification of glycoside hydrolase family 5 (GH5), BMC Evol. Biol. 12 (2012) 186.
[37] W. Wang, T. Archbold, J.S. Lam, M.S. Kimber, M.Z. Fan, A processive endoglucanase with multi-substrate specificity is characterized from porcine gut microbiota, Sci. Rep. (2019) 1–13.
[38] S. Ding, How does plant cell wall nanoscale architecture correlate with enzymatic digestibility, Science 338 (2012) 1055–1060.
[39] K. Naganagouda, P.V. Salimath, V.H. Mulimani, Purification and characterization of endo-β-1,4 mannanase from *Aspergillus niger* gr for application in food processing industry, J. Microbiol. Biotechnol. 19 (2009) 1184–1190.
[40] W. Wang, G. Mai-Gisondi, P.J. Stogios, A. Kaur, X. Xu, H. Cui, O. Turunen, A. Savchenko, E.R. Master, Elucidation of the molecular basis for arabinoxylan-debranching activity of a thermostable family GH62 α-L-arabinofuranosidase from *Streptomyces thermoviolaceus*, Appl. Environ. Microbiol. 80 (2014) 5317–5329.
[41] D.F. Zielinska, F. Gnad, J.R. Wiśniewski, M. Mann, Precision mapping of an *in vivo* N-glycoproteome reveals rigid topological and sequence constraints, Cell 141 (2010) 897–907.